ACCURATE PREDICTION OF INSTALLED RF PERFORMANCES OF ANTENNAS ON CUBESATS

C. Cappellin [(1)], M. M. Bilgic [(1)], J. R. de Lasson [(1)], O. Borries [(1)]

[(1)] TICRA, Landemærket 29, 1119 Copenhagen, Denmark, Email: {cc; mmb; jrdl; ob}@ticra.com

***Abstract*—A typical 3 U and 6 U CubeSat hosting antennas ranging from the low UHF to the higher Ka band are modelled in the ESTEAM software package. The antennas are inspired by recent designs published in the literature. RF performances of the antennas installed on the CubeSats are computed with the MoM/MLFMM full-wave analysis method and compared with the ones in the absence of the CubeSat platform. The results show that the RF performances are substantially changed once installed on the CubeSats, indicating that platform scattering and coupling with the neighbouring antennas must be included and accounted for already in the antenna design phase.**

I. INTRODUCTION

CubeSats made of one or multiple 10 cm X 10 cm X 10 cm units, the so-called 1 U, are the smallest satellites in the market. Their use started around twenty years ago, pushed by universities which used them as educational tools and low-cost technology demonstration platforms. Today, CubeSats, especially in their 3 U, 6 U and 12 U versions, attract the attention of investors and satellite manufacturers for two main reasons. Firstly, since they allow constellations of small satellites in LEO orbit, which can compete with the traditional large satellites in GEO orbit for telecommunication applications [1], referred to as old space. Secondly, since the low cost and short development time of designing and launching a CubeSat make space accessible to the public and open up for a multitude of new applications and services, referred to as new space, as, for example, demonstrated with two recent achievements of NASA JPL [2]-[3].

CubeSat antennas realize functions like those of traditional large satellite antennas, i.e., TT&C, payload data downlink and GNSS reception [4]. With CubeSat missions operating from 400 MHz (UHF band) up to 110 GHz (W band) [5], antennas ranging from miniaturized patches to large deployable reflectors have been designed and, in most cases, manufactured. Wideband or duaL band elements are also currently under study to reduce the total number of required antennas.

The proximity of the multiple antennas on a 3 U and 6 U CubeSat makes the coupling between the antennas and the CubeSat body stronger than on traditional large satellites. Such a coupling must therefore be included and accounted for already in the antenna design phase [5]-[6]. To do that, accurate and fast full-wave simulations are necessary to design antennas that can meet the pattern, impedance matching and bandwidth requirements, once installed on the CubeSat. Despite its importance, platform scattering on CubeSats is not widely described in the literature.

The higher-order Method of Moments (MoM) algorithm accelerated by the MLFMM solver is the core of TICRA's ESTEAM software product. ESTEAM allows to perform, on portable computers, the full-wave RF simulations of the antennas on a typical Telecommunication satellite from C to Ka band [7] and is thus considered the industry standard for platform scattering in the old space sector.

The purpose of the present paper is to show that the ESTEAM software perfectly fits the needs of the new space market as well and may become an essential tool for the antenna designer working with next generation CubeSats.

Section II describes the full-wave RF modelling of a 3 U CubeSat hosting 4 UHF dipoles, a patch antenna and a helix antenna. Section III focuses on the full wave modelling of a 6 U CubeSat hosting a reflector antenna, a patch antenna and solar panels. Conclusions are finally drawn in Section IV.

II. 3 U CUBESAT MODEL

The 3 U CubeSat modelled in this work is inspired by the GOMX-3 satellite, developed by GomSpace and ESA and launched in 2015 [8]. The purpose of the satellite was to demonstrate reception of aircraft ADS-B (Automatic Dependent Surveillance-Broadcast) signals and measurement of the signal quality of geostationary telecommunication satellites in L band.

GOMX-3 hosted five antennas, see Fig. 1: A deployable helix antenna to measure the ADS-B signals, four UHF monopoles to establish communication in the initial stages after deployment, a Global Positioning System (GPS) antenna to keep track of the satellite orbit, an L band antenna to measure the quality of service supplied by the L band GEO communication satellites, and an X band transmitter patch antenna. All antennas operate in circular polarization, the first four were designed by GomSpace, while the X band patch was developed by Syrlinks. The helix and the UHF antennas were based on designs used in previous missions, while

the L band, X-band and GPS antennas were developed specifically for GOMX-3.

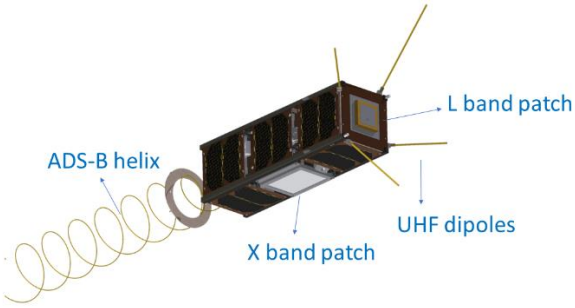

Fig. 1. GOMX-3 satellite from GomSpace. The GPS antenna is on the lateral face and not clearly visible in this picture.

The L band patch antenna designed by GomSpace is visible on the left side of Fig. 2, located on the 10 cm x 10 cm face of the satellite. The patch works in the [1.525:1.565] GHz band and is located on a high dielectric substrate with high permittivity, in order to reduce the side length of the patch to 36 mm. The excitation is through a coaxial cable. A slot in the centre and corner truncations in the patch rim are introduced to obtain circular polarization with axial ratio of less than 6 dB. The cut-outs on the side edges of the patch increase the impedance bandwidth to have a RL of around 15 dB and a near constant gain around 5.5 dBc in the desired frequency band [8].

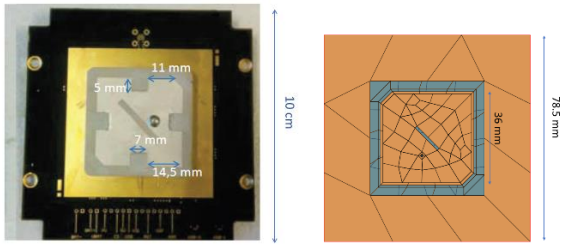

Fig. 2. L band patch antenna: On the left the antenna designed and manufactured by GomSpace for GOMX-3 [8], and on the right the antenna designed and modelled by TICRA for the present work.

The L band patch antenna modelled by TICRA in this work is shown on the right side of Fig. 2. The patch has the same size length of 36 mm and uses a dielectric with permittivity equal to 7. The antenna is modelled in TICRA's ESTEAM product: The radiation pattern for the bare antenna (that is, in the absence of the CubeSat platform) is seen in Fig. 3. Due to the missing cut-outs in the patch rim, the band is slightly narrower: A RL of around 14 dB is achieved in the [1.525:1.555] GHz band. The axial ratio (AR) is 4 dB. As seen in Fig. 1, the patch antenna is located on the top face of the 3 U CubeSat, in between the four UHF dipoles. It is therefore interesting to compute the interaction between the patch and the dipoles, and to investigate how this affects the patch antenna pattern. The top face and the UHF dipoles are modelled in ESTEAM as a CAD file. A plot of the currents induced on the patch, dipoles and top face, when the patch is radiating and the dipoles are matched, is seen in Fig. 4. The corresponding radiation pattern is shown in Fig. 5.

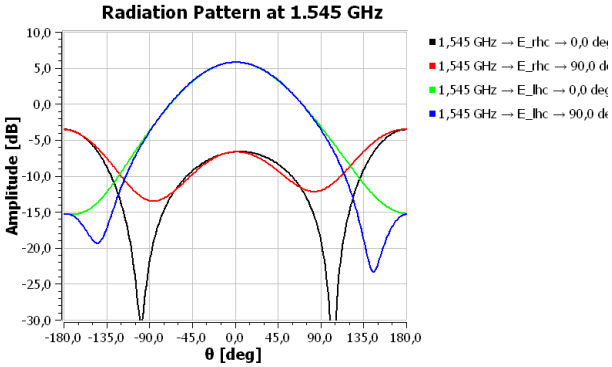

Fig. 3. Radiation pattern at 1.545 GHz of the bare L band patch antenna from TICRA.

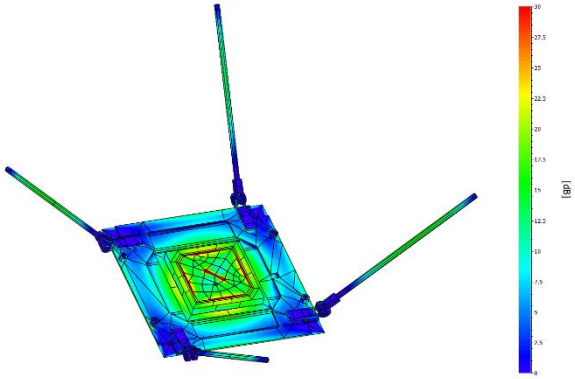

Fig. 4. Amplitude of the total electrical currents induced on the top face of the 3U CubeSat, when the L band patch is radiating and the UHF dipoles are matched.

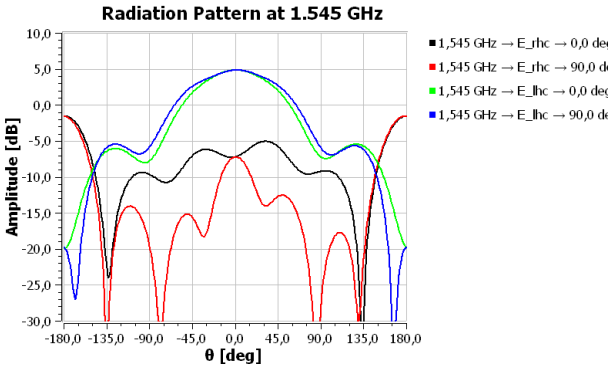

Fig. 5. Radiation pattern at 1.545 GHz of the L band patch antenna from TICRA in presence of the matched UHF dipoles and top face.

When comparing Fig. 3 with Fig. 5 it is seen that the effect of the dipoles and the top face on the patch antenna

pattern is significant. In particular, the peak drops by 0.9 dB and two sidelobes arise. The cross-polar component changes shape and the AR deteriorates by 1 dB compared to the performances of the bare patch antenna. The RL of the patch antenna is not deteriorated and remains at 19 dB. The other scattering parameters with the UHF ports are below -50 dB, indicating that the UHF and L band ports are not coupled. Fig. 6 shows the pattern of the patch antenna in presence of the matched UHF dipoles and the full 3 U CubeSat platform as dotted lines. The solid lines are those from Fig. 5. Changes are visible in the main beam for both the co-polar and the cross-polar components. It is thus concluded that the UHF dipoles and the full 3 U CubeSat influence the pattern of the L band patch antenna, when the patch antenna is radiating and the UHF dipoles are matched.

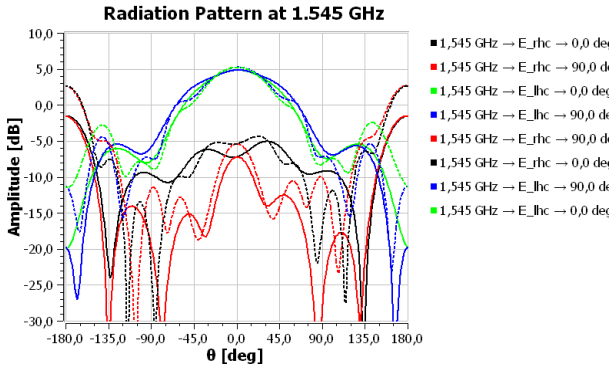

Fig. 6. Radiation pattern at 1.545 GHz of the L band patch antenna from TICRA in presence of the matched UHF dipoles (solid, same as in Fig. 5) and the full 3 U CubeSat (dashed).

A helix antenna similar to the one on GOMX-3 is finally added to the 3 U CubeSat model. The helix antenna is modelled in ESTEAM as a curved wire excited by a voltage generator. The helix has a diameter of 8.5 cm, a pitch angle of 8˚ and 6.5 turns, and works at 1.090 GHz. The pattern of the helix in presence of the 3 U CubeSat alone is shown in Fig. 7. The AR is smaller than 4 dB in the main beam. The model of the 3 U CubeSat in ESTEAM used to perform the full-wave analysis of this section is illustrated in Fig. 8.

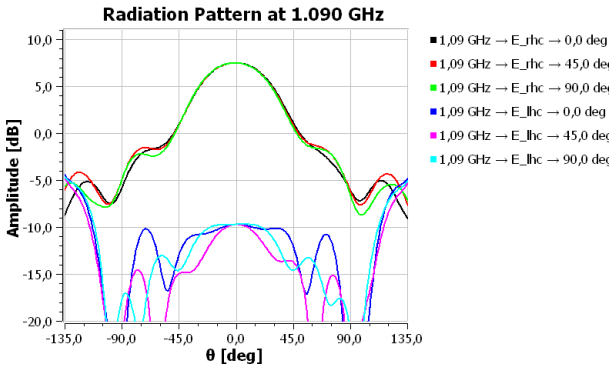

Fig. 7. Radiation pattern at 1.090 GHz of the ADS-B helix antenna in presence of the 3 U CubeSat.

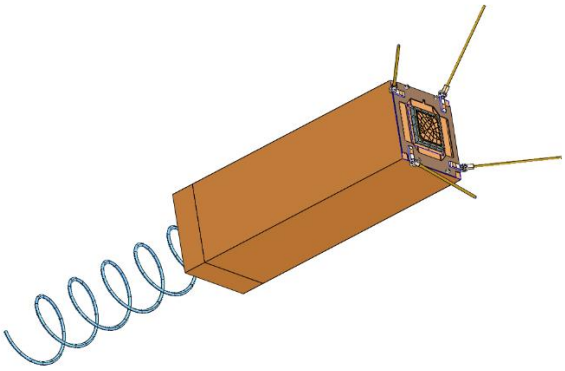

Fig. 8. Full-wave model of the 3 U CubeSat with the ADS-B helix antenna, four UHF dipoles and the L band patch used for the platform scattering analysis of Section II.

III. 6 U CubeSat Model

The 6 U CubeSat modelled in this work is inspired by the RainCube mission, developed by NASA JPL and launched in 2018 [3]. RainCube had the purpose to develop, launch and operate the first radar instrument on a 6 U CubeSat. The instrument was made by a lightweight deployable reflector antenna with a 500 mm projected aperture working at 35.75 GHz. The spacecraft is displayed in Fig. 9.

Fig. 9. The RainCube spacecraft, as available at [10].

The reflector antenna modelled by TICRA is a Cassegrain ring focus working at 33 GHz in linear polarization. The main reflector has a diameter of 500 mm and a focal length of 220 mm, while the subreflector has a diameter of 60 mm. The input waveguide radius is 3.3 mm, which ensures TE11 mode propagation in the 32-34 GHz band. A waveguide step and one conical

section are added to the input waveguide, to achieve a RL of 15 dB, as shown in Fig. 10. The subreflector has a thickness of 5 mm and is supported by three circular struts. Finally, 30 ribs are added to model the pillowing effect of the deployable reflector. The MoM/MLFMM solver of ESTEAM is used to compute the pattern of the antenna, with the associated MoM mesh shown in Fig. 11. The reflector is assumed perfect electric conducting.

Fig. 10. Details of the waveguide illuminating the subreflector.

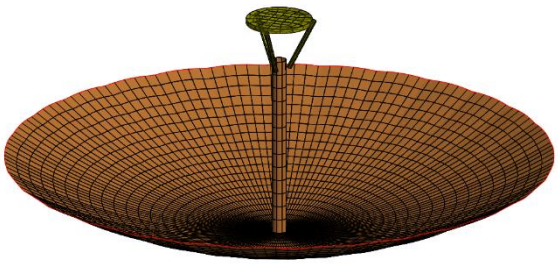

Fig. 11. MoM mesh of the reflector antenna considered for the 6 U CubeSat model of this work.

The pattern of the bare reflector antenna in free space is seen in Fig. 12. Adding solar panels and the full 6 U platform in the full wave analysis, see Fig. 13, does not affect the pattern of the reflector antenna, since the CubeSat and most of the solar panels are shadowed by the reflector surface.

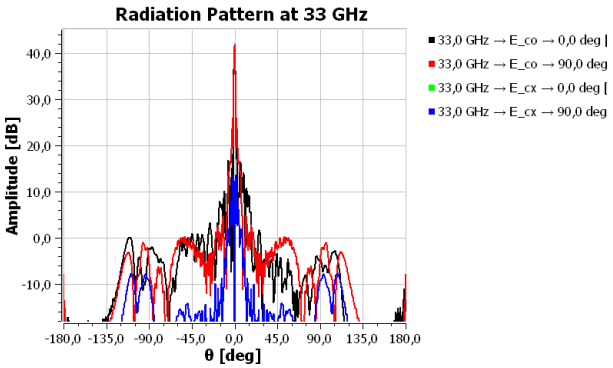

Fig. 12. Radiation pattern at 33 GHz of the bare reflector antenna of Fig. 11.

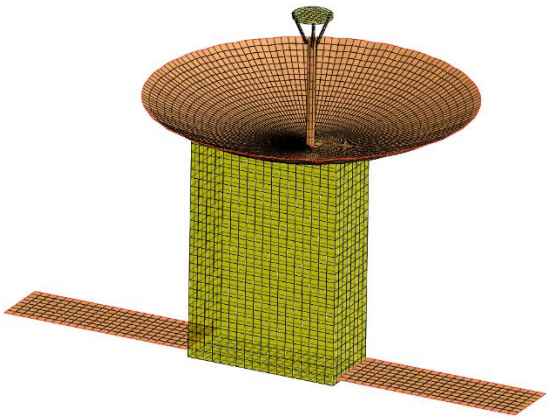

Fig. 13. MoM mesh of the reflector antenna, the 6 U CubeSat and the solar panels considered in this paper.

On the lateral side of the RainCube platform there is an S band patch antenna for ground communication and data downlink. The antenna model developed by TICRA for this work is shown in Fig. 14. The patch is squared, with a side length of 37.3 mm. It is located on a dielectric of 2.72 mm height with permittivity equal to 3, on a ground plane of 63.6 mm. A coaxial port excites the antenna in linear polarization. The pattern of the bare S band patch is shown in Fig. 15, as computed with ESTEAM.

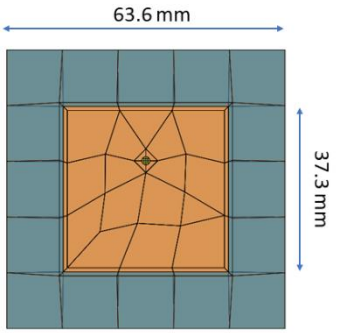

Fig. 14. S band patch antenna modelled by TICRA for this work.

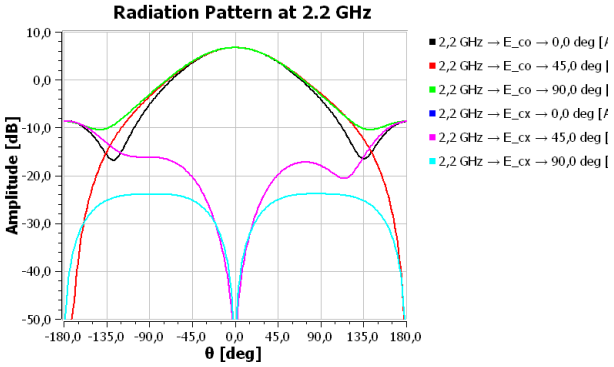

Fig. 15. Radiation pattern at 2.2 GHz of the bare patch

antenna of Fig. 14.

The pattern of the S band patch located on the side of the 6 U platform in presence of one solar panel is shown in Fig 16. When comparing Fig. 15 with Fig. 16 it is possible to see that the co- and cross-polar pattern is strongly affected by the solar panel and satellite face, especially in the φ=0˚ deg plane, which is the plane given by the two structures. The corresponding induced currents are shown in Fig. 17.

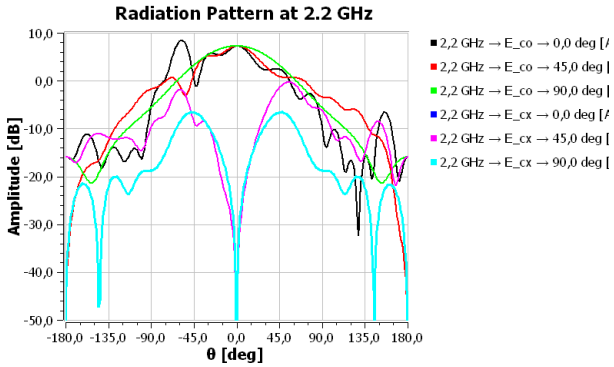

Fig. 16. Radiation pattern at 2.2 GHz of the patch antenna of Fig. 14 located on the lateral side of the 6 U platform and in presence of the solar panel.

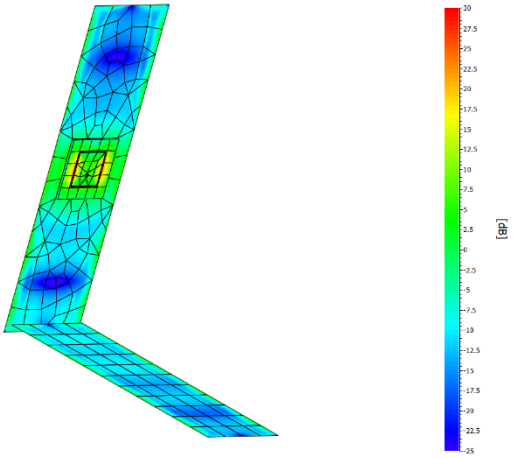

Fig. 17. Amplitude of the total electrical currents induced on the lateral face of the 6 U satellite and one solar panel, when the S band patch is radiating.

IV. CONCLUSIONS

A 3 U CubeSat, inspired by the GOMX-3 satellite of GomSpace and ESA, and a 6 U CubeSat, inspired by the RainCube satellite of NASA JPL, were modelled in the ESTEAM software package from TICRA. On the 3 U CubeSat a helix antenna working in the ADS-B band, four UHF dipoles and one L band patch antenna were considered. On the 6 U CubeSat, a reflector antenna working at 33 GHz and a patch antenna working at 2.2 GHz were analysed.

Full wave analysis was computed with the higher-order MoM algorithm accelerated by the MLFMM solver on the bare antennas and on the antennas installed on the CubeSats. The results showed that the 3 U CubeSat and the UHF dipoles strongly influenced the pattern of the L band patch antenna, when the patch antenna was radiating, and the UHF dipoles were matched. On the 6 U CubeSat, the lateral side of the satellite and the solar panel influenced the pattern of the S band patch antenna, while the pattern of the reflector antenna was not affected by them, due to the shadowing effect of the reflector.

The results show that the RF performances of the electrically small antennas are substantially changed once installed on the CubeSats, indicating that platform scattering and coupling with the neighbouring antennas must be included and accounted for already in the design phase. This work indicates that the ESTEAM software may become an essential tool for the antenna designer working with next generation CubeSats.

REFERENCES

[1] Y. Rahmat-Samii, V. Manohar, and J. M. Kovitz, “Think small, dream big: A review of recent antenna developments for CubeSats,” IEEE Antennas Propag. Mag., vol. PP, no. 99, pp. 1–1, 2017.

[2] R. E. Hodges, N. Chahat, D. J. Hoppe, and J. D. Vacchione, “A deployable high-gain antenna bound for Mars: Developing a new folded panel reflectarray for the first CubeSat mission to Mars,” IEEE Antennas. Propag. Mag., vol. 59, no. 2, pp. 39–49, April 2017.

[3] N. Chahat, R. Hodges, J. Sauder, M. Thomson, E. Peral, Y. Rahmat-Samii, “CubeSat deployable Ka-band mesh reflector antenna development for Earth science missions”, IEEE Trans. Antennas and Propagation, Vol: 64 , Issue: 6 , June 2016.

[4] S. Gao, “Antennas for modern small satellites,” IEEE Antennas Propag. Mag., vol. 51, no. 4, 2009.

[5] J. R. de Lasson, O. Borries, C. Cappellin, T. Rubæk, “High frequency Cubesat platform scattering using higher-order Method of Moments”, Proc. IEEE APS Symposium, San Diego, USA, July 2019.

[6] R. Fragnier, K. Elis, V. Laquerbe, R. Contreres, A. Bellion, B. Palacin, “Compact antennas for nano- and micro-satellites: development and future antenna needs at CNES”, Proc. 13th European Conference on Antennas and Propagation (EuCAP), Krakow, Poland, April 2019.

[7] E. Jørgensen, O. Borries, P. Meincke, M. Zhou, and N. Vesterdal, “New fast and robust modelling algorithms for electrically large antennas and platforms,” Proc. 9th European Conference on Antennas and Propagation (EuCAP), Lisbon, Portugal, April 2015.

[8] A. Tatomirescu and G. F. Pedersen, J. Christiansen and D. Gerhardt,”Antenna system for Nano-satellite mission GOMX-3”, Proc. IEEE-APS Topical Conference on Antennas and Propagation in Wireless Communications (APWC), September 2016.

[9] https://www.ticra.com/software/esteam/

[10] https://www.jpl.nasa.gov/cubesat/missions/raincube.php